Tohoku J. Exp. Med., 2008, **215**, 167-180

Comparison of 30 Immunity-Related Genes from the Common Marmoset with Orthologues from Human and Mouse

KAZUYOSHI KOHU,[1,*] EIJI YAMABE,[1,*] AYAKO MATSUZAWA,[1] DAISUKE ONDA,[1] HIROSHI SUEMIZU,[2] ERIKA SASAKI,[2] YOSHIKUNI TANIOKA,[2] HIDEO YAGITA,[3] DAISUKE SUZUKI,[4] YOSHIE KAMETANI,[4] TOSHIYUKI TAKAI,[5] ATSUSHI TOYODA,[6] SONOKO HABU[4] and MASANOBU SATAKE[1]

[1]Department of Molecular Immunology, Institute of Development, Aging and Cancer, Tohoku University, Sendai, Japan
[2]Central Institute for Experimental Animals, Kawasaki, Japan
[3]Department of Immunology, Juntendo University School of Medicine, Tokyo, Japan
[4]Department of Immunology, Tokai University School of Medicine, Isehara, Japan
[5]Department of Experimental Immunology, Institute of Development, Aging and Cancer, Tohoku University, Sendai, Japan
[6]RIKEN Genomic Sciences Center, Yokohama, Japan

In the evolution of primates, the common marmoset belongs to the new world monkey family and is distinct from the great ape family (which includes humans). In this study, we predicted the amino acid sequences of 30 immunity-related genes from the common marmoset and compared them with those from human and mouse. The domain composition of each orthologous protein was analyzed by the SMART tool and was found to be the same among the three species. A BLAST search revealed that the common marmoset and human proteins were 86% identical on average, whereas the conservation between the common marmoset and mouse or between the human and mouse was only 60%. This indicates that the common marmoset and human proteins are closely related and are similarly divergent from the mouse. We divided the 30 proteins into two categories based on the degree of conservation between the common marmoset and mouse amino acid sequences. One group included 19 proteins and had a relatively high level of conservation (68% identical), whereas the other 11 proteins were less conserved (45% identical). This suggests that these immunity-related genes do not evolve at a uniform rate. Interestingly, however, ligand/receptor pairs such as interleukin-6 and interleukin-6 receptor appear to have evolved simultaneously. ——— common marmoset; evolution; immunity-related genes; orthologues; cDNA.

Tohoku J. Exp. Med., 2008, **215** (2), 167-180.

Received April 3, 2008; revision accepted for publication April 14, 2008.

Correspondence: Masanobu Satake, M.D., Department of Molecular Immunology, Institute of Development, Aging and Cancer, Tohoku University, Seiryo-machi 4-1, Aoba-ku, Sendai 980-8575, Japan.
e-mail: satake@idac.tohoku.ac.jp
*K.K. and E.Y. contributed to the work equally.

In experimental immunology, the mouse is an outstanding laboratory model organism for a variety of reasons. Mice, like humans, are mammals and therefore observations obtained in mice can be extrapolated to humans. Moreover, several genetically identical mouse strains, such as C57Black/6 and Balb/c, have been established and gene manipulations can be made to generate transgenic or knockout lines. Mice are also advantageous because they can be maintained in a specific pathogen-free or completely germ-free environment.

Despite their similarities, mice and humans belong to different orders (rodents and primates, respectively). This difference is not negligible and can be an issue in several immunological reactions (Mestas and Hughes 2004). For example, the interleukin (IL)2/IL2 receptor system induces T lymphocyte proliferation through the same signaling pathway in both humans and mice. Although human IL2 can bind to both human and murine IL2 receptors with a similar affinity, murine IL2 cannot bind to the human IL2 receptor (Gillis et al. 1978). Such murine- or human-specific ligand-receptor interactions have been also observed for other cytokines and interleukins. Immunologists also encounter species-specificity issues when they use antibodies in experiments. For example, most of the available anti-murine CD4 monoclonal antibodies do not recognize human CD4, and vice versa, anti-human CD4 antibodies do not usually recognize murine CD4. Species-specific antibodies are also available for other CD molecules. The species-specificity in ligand-receptor interactions and monoclonal antibodies reflects the difference in the amino acid sequence of homologous proteins between mice and humans.

Callithrix jacchus (the common marmoset) is a primate model organism (Mansfield 2003). It has several experimental advantages when compared to other nonhuman primates such as its ability to easily breed in a laboratory setting. It does not transmit hazardous infectious agents and has a mild behavior. The common marmoset has become increasingly used in biomedical research in areas such as neuroscience, behavioral research, toxicology and drug development and infectious diseases.

From an evolutionary standpoint of primates, the common marmoset appears to occupy a unique position because it is a new world monkey, distinct from humans and chimpanzees. However, both the common marmoset and human belong to the same anthropoidea suborder of primates. At the upper level, primates (common marmoset and human) constitute one order distinct from that of rodents (mouse). Thus, common marmoset is expected to serve as a milestone to evaluate an evolutional distance of immunity between human and mouse. To gain an insight in such comparative immunology, we have identified and sequenced 30 prominent immunity-related *C. jacchus* genes. We have compared the predicted amino acid sequence of these genes in the common marmoset with those of mouse and human and discuss their evolutional significance.

Materials and Methods

RNA isolation

The thymus and spleen of *C. jacchus* was homogenized in Trizol reagent (Invitrogen Carlsbad, CA, USA), and RNA was extracted with chloroform. The RNA in the aqueous phase was precipitated with isopropanol and washed with ethanol. The RNA pellet was dissolved in RNase-free water and treated with RQ1 RNase-free DNase. The RNA was then mixed with phenol/chloroform and recovered by ethanol precipitation. The pellet was resuspended in RNase-free water.

cDNA synthesis and sequencing

cDNA was synthesized from 5 μg RNA using the Super Script First-Strand Synthesis System (Invitrogen). PCR was performed using LA-Taq polymerase (Takara Ohtsu) and 100 ng cDNA as a template. Each reaction consisted of 30 cycles. Every cycle contained a denaturation step at 94°C for 30 sec, an annealing step at an appropriate temperature (45 to 72°C) for 60 sec and an extension step at 72°C for 60 sec. The sequences of the forward and reverse primers used are listed in Supplementary Table 1. These primers were designed in regions where a high degree of homology between the human and mouse sequences exist. Each PCR product was run on an agarose gel and a band of the correct size was extracted from the gel and cloned in a pGEM-T vec-

tor using the TA-cloning kit (Promega Madison, WI, USA). The cDNA insert was sequenced by the dideoxy-dye-terminator method.

Forward and reverse primers were created so that the length of the amplified product was approximately 500 nucleotides. For each gene of interest, five cDNA clones were isolated and sequenced. If any discrepancies between the sequences for a particular nucleic acid position arose, the nucleic acid most often found in that position was assigned to the final sequence. If the length of the cDNA was expected to be more than 500 nucleotides, multiple pairs of primers were designed to cover its entire length. The overlapping sequences were then assembled into a contiguous sequence.

Sequence analyses

The BLAST and SMART tools were used for the homology and domain analyses, respectively (Marchler-Bauer et al. 2005; Letunic et al. 2006). The three dimensional structure of protein was predicted, using the PDFAMS (Ogata and Ueyama 2000). The student's *t*-test was employed for statistical analyses.

Results and Discusssion

We have chosen 30 immunity-related genes to study in *C. jacchus* (Table 1; Note that *CD4, CD40LG, IGHG, IFNG* and *FASLG* were not included in this study, since these sequences had been deposited at GenBank/NCBI by other groups). The chosen genes encode both membrane proteins and soluble factors. The cDNA sequence for each gene was determined in order to deduce the amino acid sequence of the open reading frame. Each sequence was registered at GenBank/NCBI and the accession number of each gene is shown in Table 1. As for *IGHM (immunoglobulin heavy chain, mu, constant region)* and *IGHE (immunoglobulin heavy chain, epsilon, constant region)*, we determined the sequences that corresponded to a constant region of the molecule but did not contain its variable portion. Since these two cDNA were partial, we did not register their sequences to the database.

The number of amino acids and the domain identity are conserved

The number of amino acid residues in each protein was calculated based on the nucleic acid sequence (Table 1) and was found to be nearly identical between the common marmoset, human and mouse (see Supplementary Table 2). We also surveyed the domain architecture of each common marmoset protein by using the SMART and BLAST (PFAM) programs (Marchler-Bauer et al. 2005; Letunic et al. 2006). The domain identity for each common marmoset protein was identical with its orthologous human and murine proteins (compare the domain composition shown in Table 1 with that in Supplementary Table 2). These findings suggest that the putative functions of the 30 common marmoset proteins examined are identical or similar with the known functions of their homologous human and murine proteins.

Amino acid sequence conservation

We next compared the amino acid sequence homology of the 30 proteins in the common marmoset, human and mouse. For each protein, the percentage of conserved amino acid residues between any two species was calculated. The degree of amino acid conservation between the common marmoset and human proteins ranged from 74% (CD86) to 98% (FCER1G, Fc IgE receptor gamma polypeptide) (Table 1) and the average for the 30 proteins examined was 86% (Table 2). In contrast, the average percentage of amino acid conservation between the common marmoset and the mouse was 60% whereas the human and mouse were 61% conserved. These percentages were significantly less than the 86% observed between common marmosets and humans ($p < 0.001$, by a student t-test). Therefore, the common marmoset and human proteins are relatively close and have diverged from the mouse at approximately the same point.

Analysis of CD8A

To exemplify the above claim, we analyzed the amino acid sequence of CD8A in the three species in further detail. The amino acid sequence of CD8A between the common marmoset and human was 84% conserved, whereas between the common marmoset and mouse and between the human and mouse it was 43% and 40% conserved, respectively (Table 1). Fig. 1A shows the

TABLE 1. Structural features of 30 immunity-related *C. jacchus* genes.

Gene symbol	Accession No.	No. of amino acid residues	Domain composition	Identical aa residues (%)		
				marmoset vs human	marmoset vs mouse	human vs mouse
CD80	EF534214	282	Ig/Ig-like/TM	84	40	40
*IL4**	EF493341	151	IL4_13	83	40	44
*IGHE**		425	Ig-like/ Ig-like/ Ig-like/ Ig-like	77	42	42
CD8A	DQ189217	235	Ig/ TM	84	43	40
*IL6**	DQ658153	212	IL6	89	43	41
CD86	EF534211	327	IgV/TM	74	43	48
*IL6R**	DQ826673	468	Ig-like/ FN3/ TM	88	47	46
*FCER1A**	EF534210	257	IgC2/Ig/TM	82	48	48
CD2	EF534206	352	TM	83	49	50
*IL4R**	DQ826671	824	SCOP:d1iarb1/FN3	85	49	52
IL17F	EF613223	163	BLAST:Pfam IL17	83	56	57
*IL2RA**	DQ520834	272	CCP/ CCP/ TM	81	59	61
CD40	DQ189221	274	TNFR/ TNFR/ TNFR/ TNFR/ TM	85	61	58
*IL2**	DQ826674	154	IL2	92	61	62
IL7R	EF534213	459	BLAST:Pfam FN3	88	62	63
IL17A	EF534212	153	BLAST:Pfam IL17	90	63	63
CD28	EF534209	220	Ig-like/TM	85	63	67
IGHM		453	Ig-like/ Ig-like/ Ig-like/ Ig-like	82	64	64
*IL5**	DQ658152	134	PFAM:IL5	83	65	69
CD19	DQ189219	558	Ig/ Ig/ TM	87	66	66
CD3E	DQ189218	198	IgC2/ TM/ ITAM	80	67	64
*IL5RA**	DQ826672	420	BLAST: FN3/ SCOP:d1egja/ TM	89	68	68
IL2RG	EF534208	368	FN3/TM	94	69	70
ITGAX	EF613221	1161	int-alpha/VWA/int-alpha/int-alpha/ intalpha/int-alpha/TM	89	69	70
IL10	DQ658154	178	IL10	89	71	73
TNF	DQ520835	232	TM/TNF	87	72	79
MS4A1	DQ189220	295	PFAM:CD20	92	74	74
IL6ST	DQ859898	915	Pfam: Lep_receptor_Ig/FN3/ FN3/ FN3/ FN3/ FN3/ TM	96	75	76
CD44	EF613222	362	LINK/TM	94	75	78
FCER1G	EF534207	86	TM/ITAM	98	89	88

Domain composition was examined by SMART and BLAST (PFAM) tools. Abbreviations of domains are Ig, immunoglobulin; TM, transmembrane; IgV, immunoglobulin variable; FN3, fibronectin 3; IgC, immunoglobulin constant; CCP, complement control protein; TNFR, tumor necrosis factor receptor; int-alpha, integrin-alpha; VWA, von Villebrand factor type A; TNF, tumor necrosis factor; LINK, hyarulonan-binding; ITAM, immune-tyrosin activation motif. Three way comparisons of each protein was done using a BLAST tool. The values indicate the degree (%) of identical amino acid residues. The genes above and below the inserted line correspond to the diverged and conserved genes, respectively. Also, the genes indicated by artenisks are ligand-receptor pairs such as *IL2* and *IL2RA*, *IL4* and *IL4R*, *IL5* and *IL5RA*, *IL6* and *IL6R*, and *IGHE* and *FCER1A*.

TABLE 2. Categorization of 30 immunity-related *C. jacchus* genes.

Gene category	Identical aa residues (% in average)		
	marmoset vs human	marmoset vs mouse	human vs mouse
		$p < 0.001$	
The total 30 genes		$p < 0.001$	
	86 ± 5.5	60 ± 13	61 ± 13
The less conserved 11 genes	83 ± 4.3	45 ± 4.8	46 ± 5.5
		$p < 0.001$	$p < 0.001$
The highly conserved 19 genes	88 ± 5.1	68 ± 7.1	69 ± 7.5

The less conseved genes include *CD80, IL4, IGHE, CD8A, IL6, CD86, IL6R, FCER1A, CD2, IL4R* and *IL17F*, whereas the highly conseved genes include the remaining 19 (see the inserted line in Table 1). A significant difference with the indicated p-value (by the student *t*-test) was detected for the bracket-indicated, pairwise comparison.

amino acid alignment and the characteristic motifs/domains found in human CD8A (Leahy et al. 1992) are indicated by bars. These domains include a signal peptide, 9 beta-strands (A to G), 3 complementary determining regions (CDR1 to CDR3), a hinge region, a transmembrane domain and a $p56^{lck}$-binding site. The beta-strands A-C′ and C″-G form beta sheets, whereas the CDRs do not have a rigid structure but rather form loose loops. The beta sheets and CDRs together constitute the immunoglobulin variable (IgV) region. The hinge region connects the IgV and transmembrane domains.

Each motif/domain of CD8A can be classified into three categories based on its degree of conservation/divergence between the three species. In the first category, the transmembrane domain and intracellular $p56^{lck}$-binding site were highly conserved between the three species. This is consistent with the notion that the transmembrane and intracellular domains evolve slowly compared to extracellular domains. The E, F and G strands were also highly conserved between the three species. In the second category, regions in CD8A including the signal sequence, the A, B, C, C′ and D strands and the CDR1 and CDR3 domains were well conserved between the common marmoset and human but distinct from the mouse. Existence and abundance of these secondly categorized motifs/domains is in line with the above described BLAST scores between the three species. The CDR2 was in the third category. The sequences of primates were drastically different from that of mouse (in this sense, the CDR2 resembles the motifs/domains of the second category), and yet those from common marmoset and human were distinct to some extent from each other (in this aspect, the CDR2 is distinct from the motifs/domains of the second category).

We simulated the three dimensional structure of the common marmoset CD8A protein with the prediction tool, PDFAMS (Ogata and Ueyama 2000) using the structure previously determined for the extracellular domain of human CD8A as a template (Leahy et al. 1992). The overall structure of common marmoset CD8A was quite similar to the human and mouse structures (data not shown). Interestingly, despite the divergence of amino acid sequences in this domain, the CDR2 had similar loop-like configurations in both the common marmoset and human (Fig. 1B). In contrast, the loop predicted for mouse CDR2 was strikingly different from the primate structures of CDR2. Thus, the amino acid sequence in the third category can actually exhibit a feature of second category from the aspect of three dimensional structure.

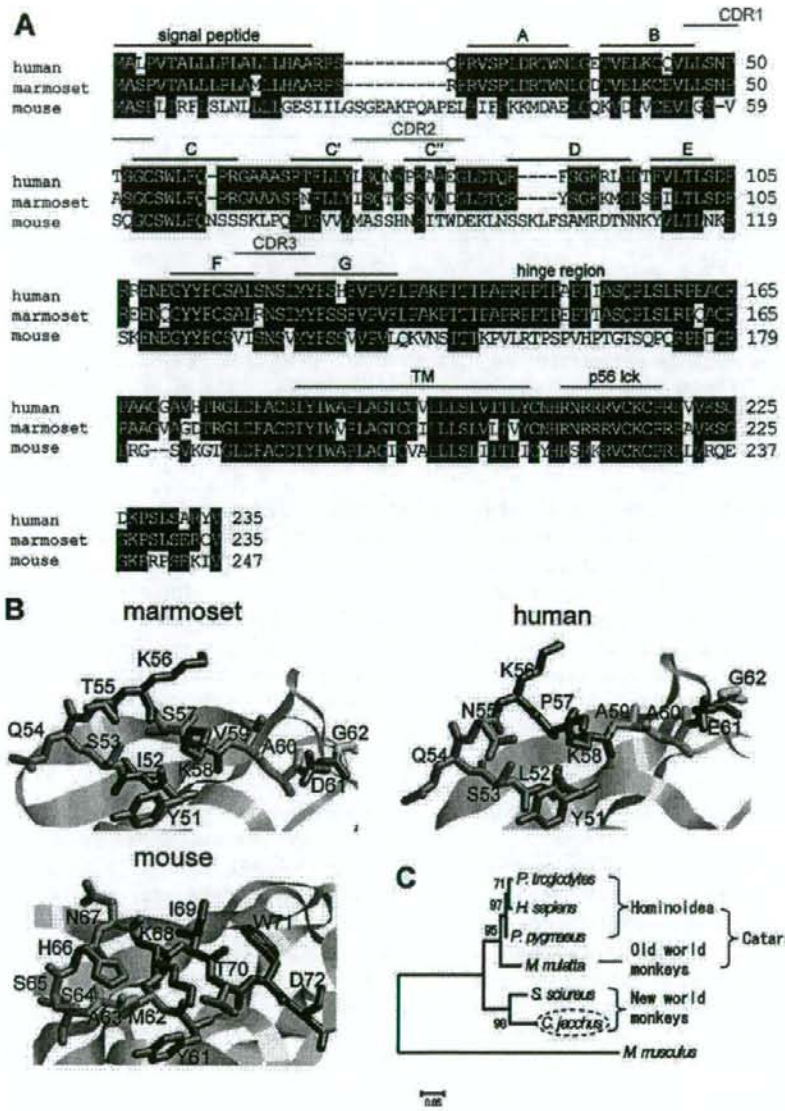
A
signal peptide
A
B
CDR1
C
C'
CDR2
C"
D
E
CDR3
F
G
hinge region
TM
p56 lck
human
marmoset
mouse
B
marmoset
human
mouse
C
P. troglodytes
H. sapiens
P. pygmaeus
M mulatta
S sciureus
C. jacchus
M musculus
Hominoidea
Old world monkeys
Catarrhini
New world monkeys

We also performed phylogenetic tree analysis of CD8A from various primates (Fig. 1C). The CD8A from the common marmoset (a new world monkey) was distinct from the *Catarrhini* and mouse.

Non-uniform evolution of immunity-related genes

In Table 2, the average percentage of amino acid conservation between the common marmoset and human was measured. We found that the standard deviation between the 30 genes was relatively low (± 5.5). This suggests that the degree of evolutional divergence between these two species does not heavily depend on the identity of the gene. In contrast, the standard deviation values between the common marmoset and mouse or between the human and mouse were as large as ± 13. Therefore, the extent of evolutional divergence from mouse to primates varies.

We crudely categorized the 30 genes into two groups (see the inserted line in Table 1) based on their conservation between species. The proteins above the inserted line were less than 60% identical between primates and mouse. The less conserved genes include *CD80, IL4, IGHE, CD8A, IL6, CD86, IL6R (IL-6R alpha), FCER1A (Fc IgE receptor, alpha polypeptide), CD2, IL4R (IL-4R alpha)* and *IL17F*. As seen in Table 2, the average number of amino acids that were identical between the common marmoset and mouse in this group were 45% ± 4.8 and whereas the percent identity between the human and mouse was 46% ± 5.5. These less conserved genes have diverged rather quickly from mouse to primates. The remaining 19 genes (below the inserted line in Table 1) were more highly conserved. The average amino acid identity in these proteins was 68% ± 7.1 between the common marmoset and mouse and 69% ± 7.5 between the human and mouse. These 19 genes appear to have diverged relatively slowly from mouse to primates. These findings suggest that these immunity-related genes evolve at non-uniform but unique rates.

The extent of conservation and/or divergence does not appear to be related to whether the protein is a membrane or soluble protein. For example, both CD44, a membrane protein, and TNF (TNF alpha), a soluble factor, were highly conserved. On the contrary, CD80, a membrane protein, and IL4, a soluble protein, were highly divergent. Furthermore, the conservation and/or divergence of a protein between species is not likely attributable to a particular domain in the protein. For example, immunoglobulin-like domains were detected in both the diverged (CD80, CD8A) and conserved (CD28, CD19) proteins.

Both *IL4* and *IL5* are Th2-type genes located in the same gene cluster. However, IL4 was highly divergent, whereas IL5 was conserved. IL4 has been previously shown to be highly divergent between the rat and the mouse, whereas IL5 was found to be conserved between these two species.

Fig. 1. Comparison of CD8A in the human, common marmoset and mouse. A: Sequence alignments from human, common marmoset and mouse CD8A proteins. Identical amino acid residues are indicated by white letters in a black background. The characteristic features in human CD8A are indicated by bars and include a signal peptide, 9 beta strands (A to G in black), 3 CDR domains (CDR1 to CDR3 in red), a hinge region, a transmembrane (TM) domain and a cytoplasmic $p56^{lck}$–binding motif. B: Comparison of the three dimensional structures of the CDR2 region. The structure of CDR2 was predicted for the common marmoset (Y51 to G62) and mouse (Y61 to D72) using the known structure of human CD8A (Y51 to G62) as a template. The amino acids numbers in B represent those in the mature protein (a signal peptide has been cleaved off from the open reading frame). C: Phylogenetic tree analysis of CD8A from various primate species. The tree was constructed by Clustal X-aligning the multiple amino acids sequences and then joining the nearest neighbors. CD8A from the common marmoset (*C. jacchus*) is encircled by a broken oval line. The numbers represent the probability of neighbor-joining, where a high number is more likely to join. The sequence sources were XP_001138871 (*P. troglodytes*), NM_001768 (*H. sapiens*), P30433 (*P. pygmaeus*), XP_001092778 (*M. mulatta*), CAB41462 (*S. sciureus*), DQ189217 (*C. jacchus*) and XM_132621 (*M. musculus*).

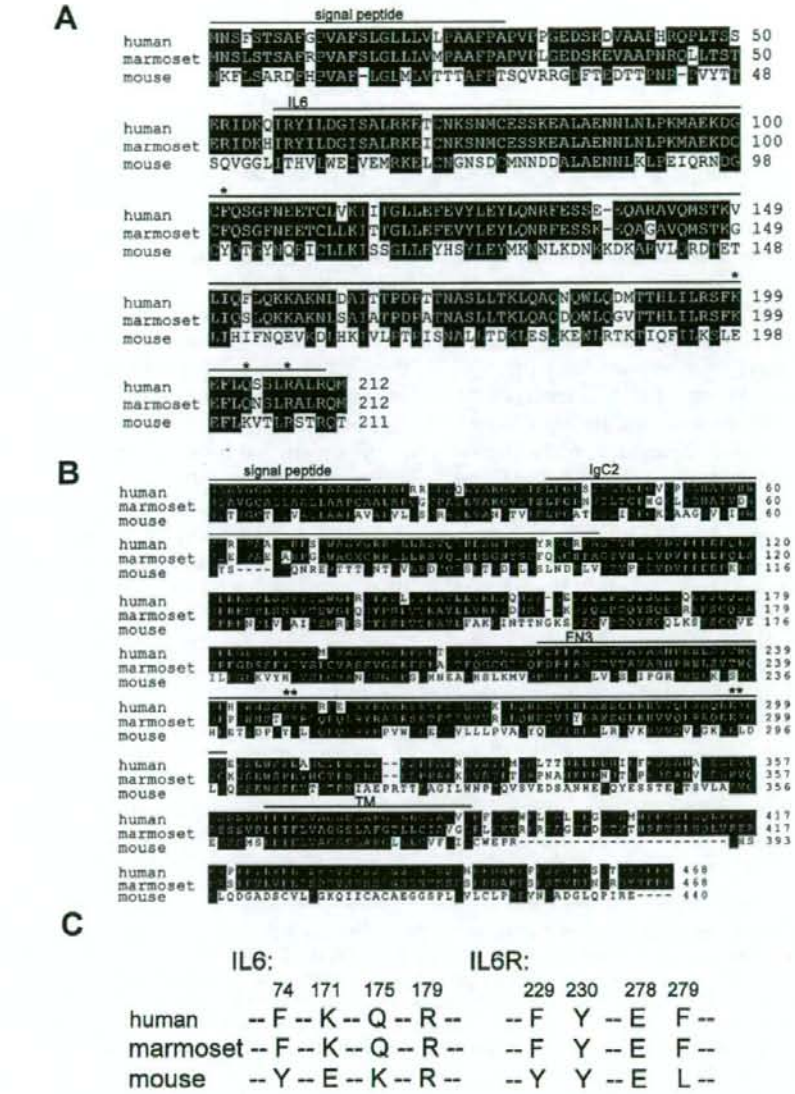

Fig. 2. Multiple alignments of IL6 (A) and IL6R (B) derived from the common marmoset, human and mouse. Identical residues are indicated by white letters in a black background. The domain structures identified by the SMART tool are indicated by bars. Ig, immunoglobulin-like; FN3, fibronectin 3, TM, transmembrane. C: The residues important for IL6-IL6R interaction (indicated by the asterisks in A and B) are aligned (note that their amino acid numbers in C are based on the signal peptide-cleaved, mature protein).

Mouse and rat IL5 are 93% identical, whereas IL4 is only 57% identical (Richter et al. 1990; Uberla et al. 1991). This suggests that a physical link in the genome does not likely influence genetic diversity between related species. The factor(s) responsible for the non-uniform evolution of genes is not clear. Mice and primates live in very different ecological niches and encounter widely different pathogens. These environmental pressures may explain why immunity-related genes have evolved so heterogeneously.

Co-evolution of ligand-receptor pairs

Among the 30 genes examined, five ligand-receptor pairs were worth mentioning (see the genes indicated by asterisks in Table 1). For each pair, the degree of amino acid conservation between primates and mouse was quite similar. For example, IL6 and IL6R were both categorized as less conserved genes and were 41-43% and 46-47% identical, respectively. In contrast, IL5 and IL5RA were both categorized as highly conserved genes and were 65-69% and 68% identical, respectively. This data supports the hypothesis that the ligand and receptor genes have co-evolved.

One of these ligand-receptor pairs, IL6 and IL6R, were investigated in more detail in Fig. 2A and B. The primates' IL6 was divergent from murine IL6 over the entire length of the protein. Likewise, the divergence in IL6R was not limited to the extracellular domain but extended throughout its cytoplasmic region (note that only the transmembranous region is highly conserved among the three species).

IL6, IL6R and IL6ST (gp130) together form a complex that is composed of 2 molecules each of IL6, IL6R and IL6ST. A crystal structure of this hexamer has been solved using human-derived proteins, and all three proteins interact directly with each other (Boulanger et al. 2003). The IL6-IL6R interaction is mediated by a site I interface and is an initial step for hexamer formation. The amino acid residues that are required for the site I interface are indicated by asterisks in Fig. 2A and B. Many of these residues are known to be vital for this interaction based on a mutation study (Kalai et al. 1997). The amino acids required for the interaction are aligned in Fig. 2C. R179 in IL6 and Y230 and E278 in IL6R were conserved among the three species, whereas F74, K171 and Q175 in IL6 and F279 in IL6R were the same in the two primates but different in the mouse. Therefore, if IL6 and IL6R co-evolved from rodents to primates, the amino acid residues responsible for the protein-protein interaction would have also co-evolved.

Conclusion

In summary, each immunity-related gene appears to evolve with its own rate from rodents to primates, and yet those that specifically belong to a ligand-receptor pair are likely to co-evolve.

Acknowledgments

We thank M. Kuji for her secretarial assistance. This work was supported in part by a research grant from the Japan Science and Technology Agency. M.S. is a participant in the 21st Century COE Program in the "Center for Innovative Therapeutic Development towards the Conquest of Signal Transduction Diseases" at Tohoku University.

References

Boulanger, M.J., Chow, D.C., Brevnova, E.E. & Garcia, K.C. (2003) Hexameric structure and assembly of the interleukin-6/IL-6 alpha-receptor/gp130 complex. *Science*, **300**, 2101-2104.

Gillis, S., Ferm, M.M., Ou, W. & Smith, K.A. (1978) T cell growth factor: parameters of production and a quantitative microassay for activity. *J. Immunol.*, **120**, 2027-2032.

Kalai, M., Montero-Julian, F.A., Grotzinger, J., Fontaine, V., Vandenbussche, P., Deschuyteneer, R., Wollmer, A., Brailly, H. & Content, J. (1997) Analysis of the human interleukin-6/human interleukin-6 receptor binding interface at the amino acid level: proposed mechanism of interaction. *Blood*, **89**, 1319-1333.

Leahy, D.J., Axel, R. & Hendrickson, W.A. (1992) Crystal structure of a soluble form of the human T cell coreceptor CD8 at 2.6 A resolution. *Cell*, **68**, 1145-1162.

Letunic, I., Copley, R.R., Pils, B., Pinkert, S., Schultz, J. & Bork, P. (2006) SMART 5: domains in the context of genomes and networks. *Nucleic Acids Res.*, **34**, D257-D260.

Mansfield, K. (2003) Marmoset models commonly used in biomedical research. *Comp. Med.*, **53**, 383-392.

Marchler-Bauer, A., Anderson, J.B., Cherukuri, P.F., DeWeese-Scott, C., Geer, L.Y., Gwadz, M., He, S., Hurwitz, D.I., Jackson, J.D., Ke, Z., Lanczycki, C.J., Liebert, C.A., Liu, C., Lu, F., Marchler, G.H, Mullokandov, M., Shoemaker, B.A., Simonyan, V., Song, J.S., Thiessen, P.A., Yamashita, R.A., Yin, J.J., Zhang, D. & Bryant, S.H. (2005) CDD: a conserved domain database for protein classification. *Nucleic*

Acids Res., **33**, D192-D196.
Mestas, J. & Hughes, C.C.W. (2004) Of mice and not men: differences between mouse and human immunology. *J. Immunol.*, **172**, 2731-2738.
Ogata, K. & Umeyama, H. (2000) An automatic homology modeling method consisting of database searches and simulated annealing. *J. Mol. Graph. Model.*, **18**, 258-272.
Richter, G., Blankenstein, T. & Diamantstein, T. (1990) Evolutionary aspects, structure, and expression of the rat interleukin 4 gene. *Cytokine*, **2**, 221-228.
Uberla, K., Li, W.Q., Qin, Z.H., Richter, G., Raabe, T., Diamantstein, T. & Blankenstein, T. (1991) The rat interleukin-5 gene: characterization and expression by retroviral gene transfer and polymerase chain reaction. *Cytokine*, **3**, 72-81.

Supplementary TABLE 1. The sequences of primers used to amplify transcripts.

Gene	forward primer (5'-3')	reverse primer (5'-3')
CD80	tttgcacctgggaagtgccctggtcttact	cctccagaggttgagcaaattatccttct
	gctgacttccctacacctagtatatctgac	agggcaaggtggggtaatcttgtccatctg
IL4	gtcagcattgcattgttagcttctc	aataaagctatcaaaaactcataaattaaa
IGHE	cctccacacagagcccatccgtctt	gtcatttaccgggatttacagacac
CD8A	RaRaacSaRggctactatttctgctc	tgaagtMatgtagtRgYtgtNgc
CD8A	tccYgSgcScctcccctMgMgcccKagctt	ttcRctKKcWgRaRgacYggcacga
IL6	aaaagatggatgcttccaatctggat	acataaattaactcagcttcacatat
IL6	ctcgagcccaccgggaacgaaagagaa	actccaaaagaccagtgatgattttca
IL6R	ggacagaatccaggagtcctccagctgaga	cgtttgtgttttatcatccacagggtccaggc
IL6R	gaagacttccaggagccgtgccagtattcc	ctgggaggcttgtcgcatttgcagaatct
IL6R	ctctgcgggaccatggagtggtagccgagg	tgtctcctccgggactgctaactggcag
IL4R	ccgcttgggcgcccggacggcgaatggagc	gaccatgtcctccatgaacaggtggcacac
IL4R	agcagtggggaagaggggtataagccttt	ccaggcatggataagccctagtcctcatct
IL4R	gctcacatgccctgggatgagttcccaagt	ggtggctccctgtccagtccaaaggtga
IL4R	gaattgtcttaccaagctcttgccctgttt	gtgcaagtcaggttgtctggactctgggtc
IL4R	gcagtcaacatttggagtgaaaacgacccg	gatctccactgggcaccatgctgattttcc
IL4R	ctcccaatggggtggctttgctctgggctc	gcggagggagggttctaggtaggtcacgtt
IL17F	gaacacaggcatacacaggaagatacattc	ggcatttctacagcttcttcagctgagtgg
IL2RA	accaagYgagccttccaggtcactgca	cttctgttgtctgttcYcggcttcttacc
IL2RA	ctgcagagaaagacctccgcttcactgccc	agcaggacctctgtgtagagccctgtat
CD40	gctacagggRtttctgataccatctgcga	cagcagcWccaggctctcYRgcca
CD40	agtggtcctgccgcctggtctcacct	ctttggtYtcacagcttgtccaagggtgac
IL2	taatcactactcacagtaacctcaactcctgc	gaaggcctgatatgttttaagtgggaagcac
IL7R	ttcatttcatacacactggctcacac	atgtcaccacaaagtcattggctccttccc
	acctgaggctccttttgacctgagtgtcgt	ctagcttgaatgtcatccaccctatgaatc
	gtgagtttcaatcctgaaagtttcctggac	cttccctttaaatcatctttgtcgctcacg
IL17A	gcaggcacaaactcatccatccccagttga	atagtctaactgctttggggagtgtgggc
IGHM	acccacacagacctgccctcgccactgaag	ggttagtttgcatgcacacacagagcggc
IGHM	gtggggtctggcgtcaccacggaccaggtg	ggttcagctgctcccgggctggtggcagca
IGHM	gccaagggaccacggtcaccgtctcctca	gatggtcagtgtgctggtcaccttgtagg
IL5	gccaaaggcaaacgcagaacgtttcagagc	aatctttggctgcaacaaaccagtttagtc
CD19	aagaRgaaggggaggSctatgaRgaRccWga	aSgaRRtccaggctRgYcacYtgRgRRtca
CD19	tattattgtcWccRWggMRRcctgaccat	cctgcYcaaggttggagtcRttctcatagaa
CD19	agYggggagMtgttccggtggaatgYtt	aaagtcacMRctgRgacYWtccaKccaccagt
CD19	atgccaYctcctcKccYYSTctYcYtcctcctctt	tctKtRgcccacacatacagctKgg
CD19	tgccccggagagtctgacca	cctctgaggacctgttcttcaggc
CD3E	gccatcttagtagagtaaccatcccg	cgattctcccatgggtccaagactag
IL5RA	gggagaaaccagtgtctgcctttccaatcc	ggatgaagcatccatacttttaagaga
IL5RA	gaatttaacttgcaccacaaacact	acatggagctcactgctgctctcacttgaa
IL5RA	atcttctgttgagtactggtcggaacaaga	aggggcatctgtgccaacaagccaggtgca

Supplementary TABLE 1. Continue.

Gene	forward primer (5'-3')	reverse primer (5'-3')
ITGAX	agtacgttggtctagctcttcctgaaacag	ggcaaagttgttgtataagatgctgcccg
	caagacaggagcaggacattgtgttcctga	aatatctttcagagcatcaaagtcctcc
	taaatgacattgcatcgaagccctcccagg	tcgctgtctacgtccacggagcagaggga
	atgaaggccgaagtcacggggactcagat	accagtccatcctgggtgaggtcttgac
	agctctcctccaggctgcagtattttgg	tagggaggccgtgaagtatctctgagcatc
	tgacccccattaccttgcgtctgaactt	tctcactgctcacattggctgtcagaagca
	ttcttggctacctttgacgtctcccccaa	caaagctgaggttgcccttcagggtgaaat
	acattcagaagaatcccgtgctggactgct	gtgcagtggttcctccccgtcaggcctgac
IL10	tgggttgccaagccttgtctgagatgatc	acagagaagctcagtaaataaatagaaatggg
IL10	ggcttgctcttgcaaaaccaaaccacaa	acctgctccacggccttgctcttgttttca
TNF	aagcctgtagcccatgttgtagcaaaccct	gcgtttgggaaggttggatgttcgtcctcc
TNF	gcaaggacagcagaggaccagctaagaggg	tcagctccacgccattggccaggagggcat
MS4A1	cctcWgagaaaaactccccatctacMcaR	gaaagtcagcatgtctcttggaag
MS4A1	ctttgggggctgtccaRatYatgaatgg	ctggaagaaggcaRagatcagcatc
MS4A1	gagagaagcattcagatgcatgacacaagg	tacataatgcctccccaSagagggtacca
MS4A1	gctacagggRtttctgataccatctgcga	cagcagcWccaggctctcYRgcca
MS4A1	agtggtcctgccgcctggtctcacct	ctttggtYtcacagcttgtccaagggtgac
IL6ST	cttcgagcactgtccagtattctaccgtgg	ctgctgaagttgtagcaggaactactagtc
IL6ST	agcatacacagatgaaggtgggaaggatgg	gatcttgagaagacttggactgacggaac
IL6ST	caccctgtatcacagactggcaacaagaaga	cacgactatggcttcaatttctccttgagc
IL6ST	gatactggagtgactggagtgaagaagc	ctgttatcaaatagcatttgctctctgc
IL6ST	tgaggtgtgagtgggatggtggaaggga	ccagaaacttggtgctttagatggtc
IL6ST	gaagtagaagacttagcttcaaatccct	aatcaggaaacttgtgtgttgcccattcag

Supplementary TABLE 2. Structural features of 30 immunity-related human and mouse genes.

Human gene	Accession No.	No. of amino acid residues	Domain composition
CD80	NM_005191	288	Ig/Pfam:C2-set_2/TM
IL4	NM_000589	153	IL4_13
IGHE	J00222	427	Ig-like/ Ig-like/ Ig-like/ Ig-like
CD8A	NM_001768	235	Ig/TM
IL6	NM_000600	212	IL6
CD86	NM_175862	329	IgV/TM
IL6R	NM_000565	468	IgC2/ FN3/ TM
FCER1A	NM_002001	257	IgC2/Ig-like/TM
CD2	NM_001767	351	Pfam:V-set/Pfam:C2-set/TM
IL4R	NM_000418	825	SCOP:d1iarb1/FN3
IL17F	NM_052872	163	Pfam:IL17
IL2RA	NM_000417	272	CCP/CCP/TM
CD40	NM_001250	277	TNFR/TNFR/TNFR/TNFR/TM
IL2	NM_000586	153	IL2
IL7R	NM_002185	459	Pfam:FN3/TM
IL17A	NM_002190	155	Pfam:IL17
CD28	NM_006139	220	TM
IGHM	BC073767	454	IgC1/IgC1/Ig-like/IgC1
IL5	NM_000879	134	PFAM:IL5
CD19	NM_001770	556	Ig/Ig/TM
CD3E	NM_000733	207	IgC2/ TM/ITAM
IL5RA	NM_175726	420	BLAST: FN3/ SCOP:d1egja/ TM
IL2RG	NM_000206	369	FN3/TM
ITGAX	NM_000887	1163	int-alpha/VWA/int-alpha/int-alpha/int-alpha/intalpha/ Pfam:integrin-alpha
IL10	NM_000572	178	IL10
TNF	NM_000594	233	TM/TNF
MS4A1	NM_152866	297	PFAM: CD20
IL6ST	NM_002184	918	Pfam: Lep_receptor_Ig/ FN3/ FN3/ FN3/ FN3/ TM
CD44	NM_001001391	361	LINK/TM
FCER1G	NM_004106	86	TM/ITAM

Supplementary TABLE 2. Continue.

Mouse gene	Accession No.	No. of amino acid residues	Domain composition
CD80	NM_009855	306	Ig/Pfam:Ig/TM Ig/Pfam:C2-set_2/TM
IL4	NM_021283	140	IL4_13
IGHE	Z27397	427	Ig-like/ Ig-like/ Ig-like/ Ig-like
CD8A	XM_132621	247	Ig/TM
IL6	NM_031168	211	IL6
CD86	NM_019388	309	IgV/TM
IL6R	NM_010559	440	IgC2/ FN3/ TM
FCER1A	NM_010184	250	Ig/Ig/TM
CD2	NM_013486	344	Pfam:V-set/Pfam:C2-set/TM
IL4R	NM_001008700	810	SCOP:d1iarb1/FN3
IL17F	NM_145856	153	BLAST:Pfam:IL17
IL2RA	NM_008367	268	CCP/CCP/TM
CD40	NM_011611	289	TNFR/TNFR/TNFR/TNFR/TM
IL2	NM_008366	169	IL2
IL7R	NM_008372	459	FN3/TM/TM
IL17A	NM_010552	158	Pfam:IL17
CD28	NM_007642	218	Ig/TM
IGHM	AJ294737	455	Ig-like/ Ig-like/ Ig-like/ Ig-like
IL5	NM_010558	133	PFAM:IL5
CD19	NM_009844	547	Ig/Ig/TM
CD3E	NM_007648	189	IgC2/TM/ITAM
IL5RA	NM_008370	415	FN3/FN3/ TM
IL2RG	NM_013563	369	FN3/TM
ITGAX	NM_021334	1169	int-alpha/VWA/int-alpha/int-alpha/int-alpha/intalpha/ Pfam:integrin-alpha
IL10	NM_010548	178	IL10
TNF	NM_013693	235	TM/TNF
MS4A1	NM_007641	291	PFAM: CD20
IL6ST	NM_010560	915	Pfam: Lep_receptor_Ig/FN3/ FN3/ FN3/ FN3/ FN3/ TM
CD44	NM_001039151	365	LINK/TM
FCER1G	NM_010185	86	TM/ITAM

Domain composition was examined by SMART and BLAST (PHAM) tools. As for the abbreviations, see the footnote of Table 1.

Hum. Reprod. Advance Access published February 27, 2009
Human Reproduction, Vol.1, No.1 pp. 1–14, 2009
doi:10.1093/humrep/dep012

human reproduction ORIGINAL ARTICLE *Embryology*

A novel embryonic stem cell line derived from the common marmoset monkey (*Callithrix jacchus*) exhibiting germ cell-like characteristics

Thomas Müller[1], Gesine Fleischmann[2,4], Katja Eildermann[1], Kerstin Mätz-Rensing[3], Peter A. Horn[4], Erika Sasaki[5], and Rüdiger Behr[1,6]

[1]Stem Cell Research Group, German Primate Center, Kellnerweg 4, 37077 Göttingen, Germany [2]Institute for Transfusion Medicine, Hannover Medical School, 30625 Hannover, Germany [3]Department of Infectious Pathology, German Primate Center, Kellnerweg 4, 37077 Göttingen, Germany [4]Institute for Transfusion Medicine, University Hospital Essen, Germany [5]Laboratory of Applied Developmental Biology, Marmoset Research Department, Central Institute for Experimental Animals, Kawasaki, Japan

[6]Correspondence address. Tel: +49-551-3851-132; Fax: +49-551-3851-288; E-mail: rbehr@dpz.eu

BACKGROUND: Embryonic stem cells (ESC) hold great promise for the treatment of degenerative diseases. However, before clinical application of ESC in cell replacement therapy can be achieved, the safety and feasibility must be extensively tested in animal models. The common marmoset monkey (*Callithrix jacchus*) is a useful preclinical non-human primate model due to its physiological similarities to human. Yet, few marmoset ESC lines exist and differences in their developmental potential remain unclear.

METHODS: Blastocysts were collected and immunosurgery was performed. cjes001 cells were tested for euploidy by karyotyping. The presence of markers for pluripotency was confirmed by immunofluorescence staining and RT–PCR. Histology of teratoma, *in vitro* differentiation and embryoid body formation revealed the differentiation potential.

RESULTS: cjes001 cells displayed a normal 46,XX karyotype. Alkaline phosphatase activity, expression of telomerase and the transcription factors OCT4, NANOG and SOX2 as well as the presence of stage-specific embryonic antigen (SSEA)-3, SSEA-4, tumor rejection antigens (TRA)-1-60, and TRA-1-81 indicated pluripotency. Teratoma formation assay displayed derivatives of all three embryonic germ layers. Upon non-directed differentiation, the cells expressed the germ cell markers *VASA*, *BOULE*, *germ cell nuclear factor* and *synaptonemal complex protein 3* and showed co-localization of VASA protein within individual cells with the germ line stem cell markers CD9, CD49f, SSEA-4 and protein gene product 9.5, respectively.

CONCLUSIONS: The cjes001 cells represent a new pluripotent ESC line with evidence for enhanced spontaneous differentiation potential into germ cells. This cjes001 line will be very valuable for comparative studies on primate ESC biology.

Key words: embryonic stem cell / common marmoset / germ cell / non-human primate / pluripotency

Introduction

Cell replacement therapy using pluripotent or multipotent stem cells holds great promise for regenerative treatment of a vast number of degenerative diseases. However, it is still disputed if embryonic stem cells (ESC), somatic stem cells or recently described induced pluripotent stem (iPS) cells are best suited for cell replacement studies in preclinical and possible future clinical applications (Meissner *et al.*, 2007; Okita *et al.*, 2007; Wernig *et al.*, 2007; Yu and Silva, 2008). This open issue needs extensive further investigation with all cell types being considered as sources for cell replacement therapies. Therefore, the safety and potential of all respective cell types have to be tested in preclinically relevant animal models.

Mouse ESC differ from non-human primate and human ESC cells with respect to cell culture requirements, morphology, physiology and gene expression, reflecting significant differences between mouse and primate embryogenesis and physiology (Fougerousse *et al.*, 2000; Ginis *et al.*, 2004; Tumpenny *et al.*, 2006). Therefore, it is of fundamental importance to study primate ESC. But beside ethical concerns as well as legal limitations in several countries using

human ESC, further doubts are related to the clinical safety of the potential therapies using pluripotent stem cells (Stojkovic *et al.*, 2004). It has to be ensured that transplanted cells are not tumorigenic and that cell replacement therapy does not cause other harmful long-term side effects. Furthermore, a real benefit from cell replacement therapy has to be demonstrated for the treated individual in preclinical studies. Since primates and mice differ significantly and several neurological diseases, such as Parkinson's or Alzheimer's disease, cannot be properly mimicked, especially with regard to their cognitive deficits, non-human primate models are of great relevance. To provide the best preclinical test systems, non-human primate disease models are needed in combination with allogenic replacement cells. This ensures that all cell–cell and cell–matrix interactions as well as all ligand–receptor interactions probably needed during cell replacement therapy properly function in the respective preclinical non-human primate disease model. Hence, although previous results from mouse ESC have provided invaluable insight in stem cell biology, the potential of clinical stem cell applications in humans must be pioneered in non-human primate species (Wolf *et al.*, 2004) such as macaques and marmoset monkeys.

The common marmoset monkey (*Callithrix jacchus*) is readily available as a non-human primate model that exhibits many physiological similarities to humans (Michel and Mahouy, 1990; Mansfield, 2003; Zuhlke and Weinbauer, 2003; Eslamboli, 2005). However, only a few ESC lines of this species exist to date. More than 10 years ago Thomson *et al.* (1996) created eight ESC lines from the common marmoset, but these lines are no longer available (J. Thomson, personal communication). We recently continued research with marmoset ESC by creating and characterizing the three lines: CMESC20, CMESC40 and CMESC52 (Sasaki *et al.*, 2005). Nevertheless, the more ESC lines from one species that are available the better, and the more profound the knowledge about a certain stem cell type from a certain species will be. For instance, human and non-human primate ESC lines diverge in their karyotype, gene expression and differentiation potential (Heins *et al.*, 2004; Chen *et al.*, 2008). To have available a broad collection of ESC lines, isolated from embryos at different developmental stages and sex, will benefit research on the spectrum of intra- and inter-cell line-specific varieties and epigenetic stability.

In this article, we established and characterized a fourth marmoset ESC line (cjes001) that could be cultivated successfully for over 24 months (passage 84). Besides the potential to develop into somatic cell types, this cell line also revealed strong potential to develop into germ cells upon spontaneous differentiation.

Materials and Methods

Recovery of blastocysts and initial culture

All procedures were carried out according to German and Japanese Animal Experimentation Law and all animal experiments in Japan were approved by the institutional animal care and use committee, and were performed in accordance with institutional guidelines. Animals were housed according to standard German and Japanese Primate Centre practice for the common marmoset. The method of blastocyst recovery has been described in detail (Sasaki *et al.*, 2005). Briefly, marmoset preimplantation embryos were recovered from adult marmosets kept in the marmoset colony at the Central Institute for Experimental Animals (Kawasaki, Japan) 8 days after putative ovulation (10.7 ± 1.3 days after prostaglandin F2α administration) by uterus-flush. Out of eight animal flushes, 15 embryos were collected and immunosurgically treated to receive 15 inner cell mass (ICMs) for further cultivation. Of these 15 ICMs, 3 could be expanded until passage 10. Two of these initial lines differentiated eventually, so that finally only the cjes001 line was established. The ratio from blastocyst to established non-human-primate embryonic cell line was in this case 15:1. cjes001 cells showed flat, packed and tight colony morphology and a high nucleus to cytoplasm ratio, corresponding to the morphology reported for other primate ESC, including humans, rhesus and cynomolgus monkeys. cjes001 cells were cultured as described (Sasaki *et al.*, 2005).

Immunosurgery and maintenance of ESC

The immunosurgery, isolation and culture of ESC lines were performed as described in detail (Sasaki *et al.*, 2005). The zona pellucida of the marmoset blastocyst was removed by digestion in 0.1% pronase in phosphate-buffered saline (PBS). To remove the trophoblast, the blastocysts were first incubated for 45 min at 37°C in 5% CO_2 with a 10-fold dilution of anti-marmoset fibroblast rabbit serum in Dulbecco's modified Eagle's medium (DMEM). After three washes with DMEM, the blastocysts were incubated with a 5-fold dilution of guinea pig complement (Invitrogen) in DMEM for 30 min at 37°C in 5% CO_2. After mechanical removal of the trophoblast by pipetting, the ICM was plated on 3500-rad γ-irradiated mouse embryonic fibroblast (MEF) feeder cells. First passaging of the ICMs was performed after 10–14 days by physical removal of the ICM outgrowth and dissociation by vigorously pipetting. The medium used in initial ESC culture contained 80% Knockout DMEM (Invitrogen) supplemented with 20% Knockout Serum Replacement (KSR; Invitrogen), 1 mM L-glutamine, 0.1 mM MEM non-essential amino acids, 0.1 mM β-mercaptoethanol (Sigma), 100 IU/ml penicillin, 100 μg/ml streptomycin sulfate, 250 ng/ml amphotericin B and 10 ng/ml leukemia inhibitory factor. Established cell lines were cultured without amphotericin B and leukemia inhibitory factor. For passaging, ESC colonies were treated with trypsin–EDTA (0.25% trypsin, 1 mM $CaCl_2$, 20% KSR in DMEM) to remove them from feeder layer, mechanically dissociated into clumps of 10–50 cells and replated on a new irradiated MEF feeder layer. To date, the ESC line cjes001 line has been maintained under these culture conditions for 24 months (passage 84).

Immunofluorescence staining

The cjes001 colonies were grown on γ-irradiated MEF cells in foil-bottom 24-well plates (Lumox™, Greiner Bio-One, Stuttgart, Germany) for 2–5 days, fixed for 30 min in 4% paraformaldehyde, 0.04% Triton X-100 and then washed twice in PBS. The staining with primary antibodies was done according to the manufacturer's recommendations. Antibodies were diluted in Tris-buffered saline supplemented with 5% bovine serum albumin. A complete list of all primary and secondary antibodies used in this study is provided in Table 1. After 16 h incubation in first antibody dilution at 4°C, cells were washed twice in PBS, incubated for another 60 min with the respective secondary antibody covalently linked to Alexa dye A488 or A568, or the streptavidin–fluorescein isothiocyanate conjugate (STAR2B). Immunofluorescent double-stainings were performed by simultaneous incubation with both primary and secondary antibodies. Images were taken on a Zeiss Axio Observer Z1 microscope. Counterstaining reagents were propidium iodine (1:10 000, 5 min) or Hoechst 33258 (Sigma-Aldrich).

Alkaline phosphatase staining

For alkaline phosphatase staining, the alkaline phosphatase staining kit (Dako Universal LSAB Kit, K0674 AP) was used according to the

Table 1 Antibodies used in the study to develop a novel embryonic stem cell line from the common marmoset monkey

Antibodies	Host	Company	Cat-No.
Anti-DDX4/MVH/VASA	Rabbit	Abcam	Ab 13840-100
Anti-VASA	Goat	R&D Systems	AF2030
Anti-CD49f (Biotin)	Rat	Biozol	313604
Anti-CD9 (Biotin)	Mouse	Serotec	MCA469B
Anti-PGP9.5	Rabbit	DAKOcytomation	Z5116
Anti-human Nanog	Goat	R&D Systems	AF1997
Anti-Oct3/4	Rabbit	Santa Cruz	SC-9081
Anti-Sox2	Rabbit	Chemicon	AB5603
Anti-β-Actin	Mouse	Sigma	A-1978
Anti-SSEA1	Mouse	Chemicon	MAB 4301
Anti-SSEA3	Rat	Chemicon	MAB 4303
Anti-SSEA4	Mouse	Chemicon	MAB 4304
Anti-TRA-1-60	Mouse	Chemicon	MAB 4360
Anti-TRA-1-81	Mouse	Chemicon	MAB 4381
Anti-AFP	Mouse	Sigma	A-8452
Anti-Brachyury	Goat	R&D Systems	A-F2085
Anti-β-tubulin III	Mouse	Sigma	T-8660
Alexa fluor 488 mouse	Goat	Invitrogen	A-11029
Alexa fluor 488 goat	Donkey	Molecular probes	A-11055
Alexa fluor 488 rabbit	Goat	Invitrogen	A-110034
Alexa fluor 568 mouse	Goat	Invitrogen	A-11004
Alexa fluor 568 goat	Donkey	Molecular probes	A-11057
Streptavidin-FITC		Serotec	STAR2B

PGP9.5, protein gene product 9.5; SSEA, stage-specific embryonic antigen; TRA, tumor rejection antigen; AFP, α-Fetoprotein; FITC, fluorescein isothiocyanate.

manufacturer's instructions. For histochemistry, cells were fixed with 4% paraformaldehyde for 30 s, washed twice in PBS and incubated with Fuchsin as substrate for 30 min at room temperature.

Karyotypic analysis

Confluent ESC colonies were incubated for 4 h in ESC medium containing 0.02 μg/ml Colcemid (Invitrogen GmbH, Karlsruhe, Germany), and then washed once with PBS and trypsinized (15 min, 37°C). After detaching, the colonies were centrifuged (200g, 10 min) and the pellet was resuspended in 3 ml of prewarmed (37°C) 8 mM KCl/15 mM sodium citrate solution for 25 min at room temperature. After centrifugation (200g, 10 min), 2 ml of the KCl/sodium citrate solution was removed and 4 ml ice-cold MetOH/acetic acid (3:1) slowly added to the vial. After 5 min incubation at room temperature, the cells were pelleted again (200g, 10 min), 4.5 ml of supernatant removed, the remaining liquid carefully dropped on glass cover slips and dried overnight. For Giemsa staining [Sigma, 0.4% (w/v) in buffered methanol solution, pH 6.8], the dye was added for 2 min on the coverslip, then washed 10 times with aq. bidest and dried again. For chromosome analysis, the cells were incubated after fixation on the coverslips for 5 min in McIlvaine-buffer (pH 4.6) including 0.01 μg /ml fluorescence dye (Hoechst 33258, Sigma), then washed 10 times with aq. bidest. McIlvaine-buffer containing 5 μg/ml Quinacrine mustard (Sigma Q2876) was added for 20 min. After the second staining, the cells were washed again 10 times with aq. bidest, incubated for 5 min in McIlvaine-buffer again and embedded in mounting media (Citifluor Ltd, London, UK). The chromosome analysis was performed with a Leica CW 4000 system with a modified chromosome template based on data from Sherlock *et al.* (1996).

Telomerase detection

cjes001 telomerase activity was determined by Biomax Telomerase detection kit (Biomax Inc., Ijamsville, MD, USA) according to the manufacturer's references. Telomerase from the cell extract adds telomeric repeats onto a substrate oligonucleotide and the resultant extended product is subsequently amplified by PCR (http://www.biomax.us). Briefly, 1×10^6 cjes01 cells were lysed and the cell extract was added to a quantitative telomerase determination pre-mix in a real-time PCR reaction utilizing SYBR green for 37 cycles. As controls, MEFs, immortal green monkey kidney cells (COS7) and SYBR green, exclusive of cell extract, were used.

Reverse transcriptase–polymerase chain reaction

RNA from cjes001 or teratoma was isolated by RNeasy kit (Qiagen, Hilden, Germany) according to the manufacturer's recommendation. First-strand complementary DNA (cDNA) was synthesized with Omniscipt RT Polymerase (Qiagen) and cDNA was amplified in 35 cycles (denaturation 95°C 1 min/annealing 60°C 30 s/elongation 72°C 60 s) with 2.5 U BiothermStar *TAQ* Polymerase (Genecraft, Luedinghausen, Germany) in PCR reaction buffer [160 mM $(NH_4)2SO_4$, 670 mM Tris–HCl, pH 8.8, 15 mM $MgCl_2$, 0.1% Tween 20], 0.2 mM dNTP and 0.5 mM of each primer. cDNA from MEF cells and mock reverse transcription without RT provided negative controls. A complete list of oligonucleotides used in this study is shown in Table II. If marmoset DNA sequences were unavailable, the expected sizes of the PCR products were deduced from alignments of the homologous human and mouse sequences. Selected RT–PCR products were verified by DNA sequencing (data not shown). Normal monkey tissues exhibiting considerable expression of the respective genes served as positive controls.

Embryoid body formation

To study embryoid body (EB) formation, undifferentiated ESC were removed from the MEF layer by graduated trypsination using 0.25% trypsin that was supplemented with 1 mM $CaCl_2$ and 20% KSR until the colonies detached from the feeder layer, further dissociated using 0.25% trypsin in PBS with 20% KSR and 1 mM $CaCl_2$, and cultured in hanging drop cultures for 14–20 days in DMEM (10% fetal bovine serum) with a medium change every 3 days. The EBs were frozen in OCT Compound (Tissue-Tek, Sakura Finetek Europe B.V., Zoeterwoude, The Netherlands) for cryosections, prepared for semi-thin sections according to previously published protocols (Godmann *et al.*, 2008) or used in parallel for RT–PCR.

In vivo differentiation analysis and histology of teratoma

Eight weeks after subcutaneous injection of $1–3 \times 10^6$ cjes001 cells, tumor formation could be observed in non-obese diabetic/severely compromised immunodeficient (NOD/SCID) mice. The tumors were resected from the mice, fixed in Bouin's fixative (0.9% picric acid, 9.6% formaldehyde and 4.8% acetic acid) for 5 h, further treated according to standard histological protocols for paraffin-embedded tissues and sectioned at 5 μm for hematoxylin and eosin staining. Parts of the tumor were snap-frozen in liquid nitrogen for RNA analysis. RT–PCR analysis was performed as described above. As a positive control for teratoma formation,

Table II Primers used and their respective PCR fragment sizes

Name	Primer	Annealing temperature (°C)	Expected PCR product (bp)
AFP	5′-CAGAAAYACATCSAGGAG AG-3′ 5′-GAGCTTGGCACAGATCCTTG-3′	58	390
BexRex	5′-ACA GGC AAG GAT GAG AGA AG-3′ 5′-CCC ACG TAA ACA AGT GAC AG-3′	60	269
Boule	5′-GCGACGCAAACATCAAACCAG-3′ 5′-GAACACATCCACCATCCTGTG-3′	58	187
Brachyury	5′-CTGCYTAYCAGAAYGAGGAGA-3′ 5′-GGTTGGAGARTTGTTCCGATG-3′	58	299
CD34	5′-AGCCT-GTCACCTGGAAATGC-3′ 5′-CGTGTTGTCTTGCT-GAATGGC-3′	60	627
DAZL	5′-CCAGTCCTCATCAGCTGCAAC-3′ 5′-CAACATAGCTCCTTTGCTCCC-3′	58	306
FoxD3	5′-CGACGAC-GGGCTGGAGGAGAA-3′ 5′-ATGAGCGCGATGTAC-GAGTA-3′	60	356
GCNF (hs)	5′-GGT GAT AGT GAC CAC AGT TCC-3′ 5′-CTG CTT GCT GTA AAC GGT GAG-3′	60	501
Nanog	5′-A A ACAGAAGACCAGAACTGTG-3′ 5′-AGTTGTTTTTCTGCCACCTCT-3′	60	190
Nestin	5′-GCCCTGACCACTCCAGTTTA-3′ 5′-GGAGTCCTGGATTTCCTTCC-3′	60	200
Oct3/4	5′-CCTGGGGGTTCTATTTGGGA-3′ 5′-TTTGAATGCATGGGAGAGCC-3′	60	530
SCP3 (hs)	5′-CAG GAA ATC TGG GAA GCC GTC-3′ 5′-CTT CCG AAC ACT TGC TAT CTC-3′	60	660
Sox2	5′-AGAACCCCAAGATGCACAAC-3′ 5′-GGGCAGCGTGTACTTATCCT-3′	60	200
β-Actin	5′-CATG GAGAAGATCTG GCACCAC-3′ 5′-GATCTCCTTCTGCATCCTGTC-3′	58	689
βIII tubulin	5′-CATGTCCATGAAGGAGGTGGA-3′ 5′-GTGAACTCCATCTCATCCATG-3′	58	260
Vasa	5′-TTG GGA CTT GTG TAA GAG CTG-3′ 5′-CCC GAT CAC CAT GAA TAC TTG-3′	58	554

DAZL, deleted in azoospermia-like; GCNF, germ cell nuclear factor; SCP3, synaptonemal complex protein 3.

murine ESC were utilized, whereas PBS was injected for the negative control.

In vitro differentiation

To spontaneously differentiate the cjes001 cells, the colonies were removed from the MEF layer by trypsinization, dissociated using 0.25% trypsin in PBS with 20% KSR and 1 mM $CaCl_2$, and cultured on gelatin-coated petri dishes (Nunc) in MEF-medium. After 7–10 days, the cells had lost their characteristic undifferentiated morphology and were collected for RT–PCR or analyzed by immunofluorescence staining as described above.

Western blot analysis

Western blot analysis was performed as described (Quintana *et al.*, 1993). Briefly, about 50 mg of testis tissue or stem cell culture material was mechanically homogenized (3× 30 s) in 2.5 ml IMP buffer [0.15 M NaCl, 20 mM HEPES, 1 mM EDTA and a protease inhibitor cocktail 1:10 (Sigma #P8340), at pH 7.4] using a tissue homogenizer, centrifuged (10 min, 750 g, 4°C) and resuspended in 2.5 ml lysis buffer (IMP buffer + 0.5% Nonidet P40). The protein content was determined by BCA protein assay kit (Novagen #71285-3) and equal amounts of protein per lane were loaded onto a sodium dodecyl sulfate gel. A protein marker (Novex sharp prestained protein standard, Invitrogen) served as size standard. After electrophoresis, the gel content was transferred to a polyvinylidene difluoride membrane (Amersham Hybond-P) in an electrophoresis chamber (Roth, 100 V, 1.2 h, 300 mA). The membrane was washed in PBS, incubated for 1 h in blocking solution and stained with the primary antibody (1:500) overnight (4°C). After 3 × 5 min washes in PBS, the secondary, horse-radish peroxidase conjugated antibody (1:10 000) was added for 1 h and again washed 2 × 15 min. The detection was carried out with an enhanced chemiluminescence kit (Amersham #RPN2209) in an Ecomaxx X-ray Film developer.

Results

cjes001 shows typical ESC morphology and a normal karyotype

Out of 15 ICM initially cultured, the cjes001 line was established. This line conserved its typical ESC morphology (Fig. 1A and see Sasaki

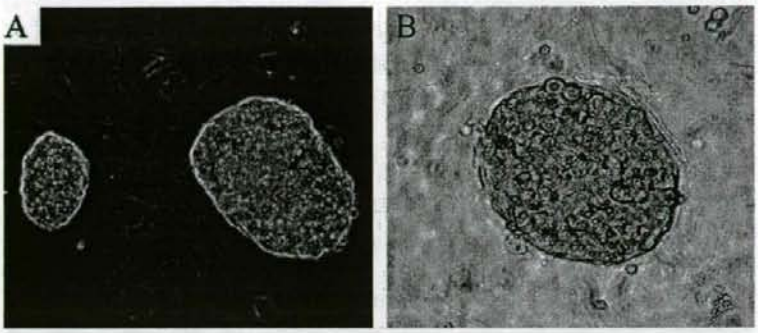

Figure 1 (**A**) Light microscopy shows tightly packed cell colonies with distinct boundaries. (**B**) Positive staining for alkaline phosphatase.

et al., 2005) and marker expression for 24 months (84 passages) and remained positive for alkaline phosphatase (Fig. 1B). The doubling time of cjes001 monitored by 5-bromo-2-deoxyuridine was roughly 19 h (data not shown). Karyotyping analysis after 64 passages showed a regular 46, XX chromosome set (Fig. 2).

cjes001 cells express undifferentiated ESC marker molecules

Immunofluorescence staining revealed the expression of the transcription factors OCT4, NANOG and SOX2 (Fig. 3), which serve as markers for pluripotency of undifferentiated ESC (Boyer *et al.*, 2005). All factors localized to the nucleus. Upon spontaneous differentiation of marmoset ESC, the expression of the pluripotency markers OCT4 and NANOG is greatly diminished at the mRNA level but not completely abolished, whereas SOX2 could not be detected in differentiated cells by RT–PCR (Fig. 4). The pluripotent cell surface antigens (Lanctot *et al.*, 2007) stage-specific embryonic antigen (SSEA)-3 and SSEA-4 (Fig. 5A–I) and keratan sulfate (tumor rejection) antigens TRA-1-60 and TRA-1-81 (Fig. 6A–F) were also strongly expressed by undifferentiated ESC. Quantitative real-time PCR analysis showed high levels of telomerase activity. The detected activities were 5-fold higher than in highly proliferative MEFs and approximately twice as high as in the SV40 virus-mediated immortalized monkey control cell line COS7 (Fig. 7).

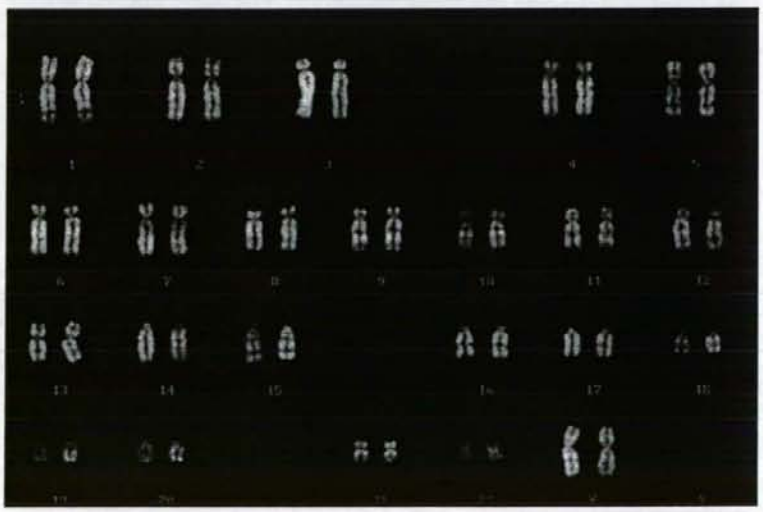

Figure 2 cjes001 cells exhibit a normal 46, XX karyotype after 64 passages.

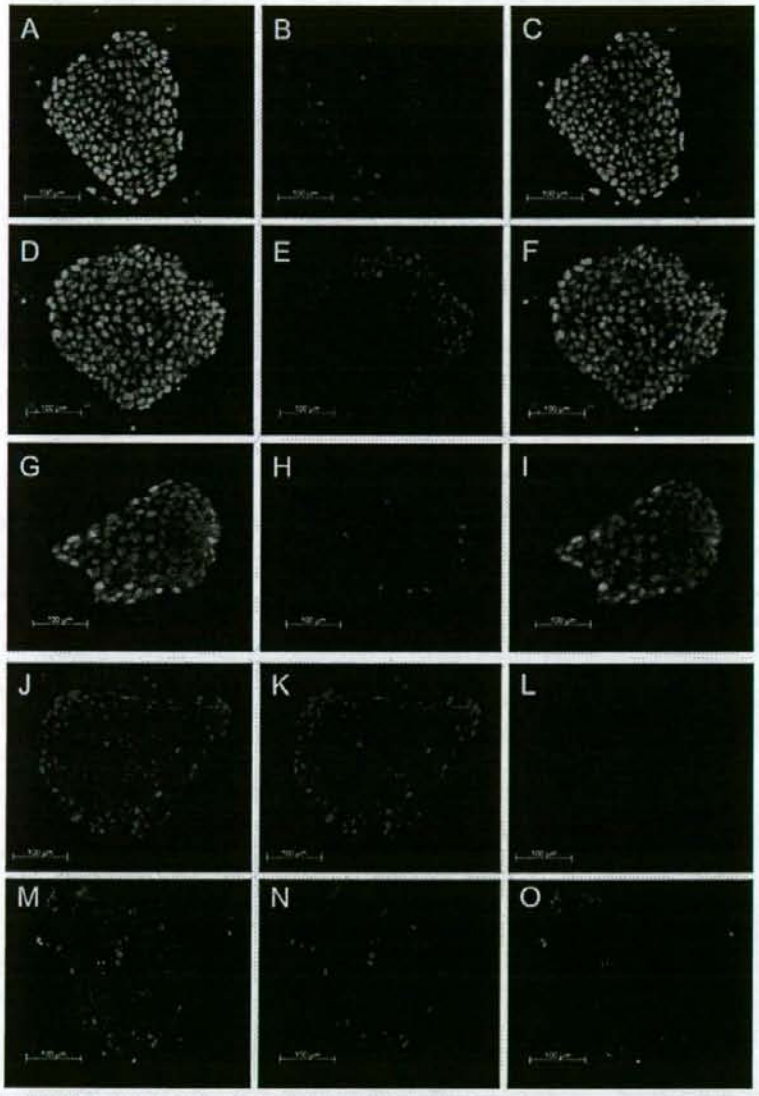

Figure 3 Immunofluorescent detection of the transcription factors OCT4 (**A**–**C**), NANOG (**D**–**F**) and SOX2 (**G**–**I**).

B, E and H show red nuclear counterstaining using propidium iodide (PI); C, F and I show green Alexa 488 staining of the respective specific antigen. A, D and G show the merged pictures. All proteins were detected in the nucleus. **J**–**L** show the negative control for the detection of NANOG staining omitting the first antibody which was generated in goat and **M**–**O** the corresponding negative control for OCT4 and SOX2. The respective first antibodies were both generated in rabbit.

cjes001 cells can form different types of EB and teratoma

As shown in Fig. 8, cjes001 cells can form cystic as well as compact types of EB. Both developed to a size of ~1.000 μm in diameter. Immunofluorescent detection of germ layer markers on cryosections of compact type EBs revealed the presence of Brachyury (mesoderm), α-Fetoprotein (AFP, endoderm) and βIII tubulin (ectoderm). Semi-thin sections showed that the wall of the cystic bodies consisted of a flattened epithelium, whose apical surface was oriented to the lumen of the cyst (right surface of the tissue string in Fig. 8F).